APPENDIX B: LAMINAR AND TURBULENT FLAME PROPAGATION IN HYDROGEN-AIR–CARBON DIOXIDE MIXTURES AND DETONABILITY OF HYDROGEN-CONTAINING GASEOUS MIXTURES*

B.1 Laminar and Turbulent Flames in H_2-Air-CO_2 Mixtures

Appendix B presents experimental data and numerical predictions on burning velocities in lean hydrogen-air-carbon dioxide premixed flames at pressures ranging from 1 to 5 bar . The effect of pressure on the laminar and turbulent combustion has been studied using the spherical bomb method.

B.2 Laminar Premixed Flames

Research on laminar flame propagation in H_2-air-CO_2 mixtures is motivated by its applications in suppression of the explosion. In this investigation, the constant-volume bomb technique is used to determine the effect of CO_2 dilution on burning velocities and flammability limits in ternary mixtures of hydrogen, air, and carbon dioxide. Data on the laminar burning velocities may by used in computer codes for the calculation of dynamic pressures generated by turbulent flames. Moreover, we want to verify the possibility of numerical predictions of the laminar burning velocities at normal and elevated pressure and temperature conditions using the model of spherical flame propagation.

Data on the burning velocities of more reactive H_2-air-CO_2 mixtures were obtained using the method of a mathematical processing of pressure-time records [B.1, B.2].Listed in Table B.2-1 are some characteristic data on the laminar burning velocities in hydrogen-air mixtures diluted with carbon dioxide.. As can be seen from the table, a significant reduction in the burning velocity results when the CO_2 dilution takes place. The pressure influence on the burning velocity is weak.

B.3 Comparison Between Measured and Computed Data on Laminar Burning Velocities

B.3.1 Effect of Dilution with CO_2

Shown in Figure B.3.1-1 are the experimental data on the burning velocities measured in a spherical bomb by p(t) and r(t) methods for the lean H_2-air mixtures ($\phi = 0.39$, 0.26, and 0.21) diluted with different amounts of CO_2. Mixture compositions are written here as

$$xCO_2 + (100 - x)\,[yH_2 + (1 - y)air],\ \phi = 2.38\,y / (1 - y)\ ,$$

where xCO_2 is the percentage CO_2, and y is the mole fraction of H_2 in an undiluted H_2-air mixture.

Numerical results are shown by solid lines. On the lower portion of the Figure B.3.1-1, the influence. of a dilution with CO_2 is illustrated in the form of the relative burning velocity S_u / S_{uo}, where S_{uo} is the burning velocity for undiluted mixtures ($x = 0$), and the equivalence ratio f is a parameter. This parameter varies from $\phi = 1$ (stoichiometric mixtures) to $\phi = 0.21$.

---

* Professor Boris E. Gelfand is the lead author of Appendix B.

As is evident from the graphs, the burning velocity depends on the values of f and f decreasing with a dilution. The relative value of the burning velocity decreases slower in the case of stoichiometric mixtures. Measured burning velocities are in close agreement with predicted ones.

B.3.2 *Effect of Pressure*

Figure B.3.2-1 shows the influence of initial pressure on the burning velocity in lean H_2-air-CO_2 mixtures ($\phi = 0.39$ and 0.26) at two initial temperatures, 298 K and 393 K. According to the predicted results, the laminar burning velocity tends to diminish with a rise in pressure. This effect is similar to that in H_2-air-H_2O mixtures .The results show that the pressure exponent is negative at the overall range of pressure and temperature investigated here. Table B.3.2-1 lists the pressure exponents for lean hydrogen-air mixtures diluted with different amounts of carbon dioxide.

It can be seen in Table B.3.2-1 that the pressure exponent does not depend on temperature at the range of pressure from 1 to 3 bar and that it decreases with pressure rise. In the range of pressure 3 to 5 bar, the pressure exponent for the H_2-air mixtures ($\phi = 0.39$) diluted with 20% CO_2 at 298 K (-0.72) is higher in absolute value than that at 393 K (- 0.59). Similar behaviour may be observed for the leaner mixture ($\phi = 0.26$) diluted with 5% CO_2.

B. 3. 3 *Effect of Temperature*

Temperature dependence of the burning velocity in H_2-air-CO_2 mixtures at the range between 298 K and 473 K is illustrated in Figure B.3.3-1. We calculated the burning velocities at 1, 3, and 5 bars of initial pressure for H_2-air mixtures ($\phi = 0.39$) diluted with 10% CO_2 and 20% CO_2 and for H_2-air mixtures ($\phi = 0.26$) diluted with 5% CO_2. As is evident from the graphs, the burning velocity increases gradually with temperature. This dependence may be described by a power function $S_u = S_{uo}(T / T_o)\ \alpha$, where a is referred to as temperature exponent. T_o = 298 K is the standard temperature, and S_{uo} is the burning velocity at 298 K.

As can be seen (Table B.3.3-1), the temperature exponent depends on the mixture composition. It is higher for the mixtures with a low reactivity ($\phi = 0.26$). The temperature exponent depends only slightly on pressure. Figure B.3.3-1shows the experimental data obtained by the method of pressure-time records in the explosion bomb at 3 and 5 bar. The influence of temperature on the burning velocity is similar to that obtained by computer simulation, but the measured burning velocities are higher than the computed burning velocities. The reason is that the influence of surface disturbances increases with pressure. In the model, the flame surface is accepted to be both smooth and spherical.

B.4 Turbulent Flames in H_2-Air-CO_2 Mixtures

The turbulent combustion rates of hydrogen-air and hydrogen-air-steam mixtures at the range of pressure and temperature relevant to the accident conditions have been investigated.. Experiments were conducted in a 2.5-L near-spherical explosion bomb. Turbulence was produced by four identical fans with rotational speeds up to 6000 rpm. The turbulent intensity ($U'\Sigma$) ranged up to about 10 m/s and was measured by a thermoanemometer . Non-homogenity of the turbulent intensity did not exceed 20%. During the flame propagation, pressure was measured with a high-sensitivity piezoelectric transducer mounted in the bomb wall. Shown in Figure B.4-1 are the experimental data on the dependence of the turbulent combustion rates S_T as a function of the turbulent intensity *U¢s* measured for hydrogen-air mixtures ($\phi = 0.39$) diluted with various amounts of carbon dioxide up to 36% by volume. The influence of initial pressure is investigated by comparison of experimental data at 1 and 5 bar. These data are obtained at room temperature.

Figure B.4-2 shows the turbulent combustion rates S_T measured in the lean hydrogen-air-carbon dioxide mixtures ($\phi = 0.26$ and $\phi = 0.21$) as a function of the turbulent intensity *U¢s* at atmospheric and elevated 3 bar pressure at room temperature. For comparison, the results of measurements of S_T in undiluted hydrogen-air mixtures at the same equivalence ratios $\phi = 0.26$ and $\phi = 0.21$ are plotted.

As would be expected , the turbulent combustion rates S_T far exceed the laminar burning velocities for the same mixtures. For the mixtures diluted with CO_2, the dependence of the turbulent combustion rate on the turbulence intensity has a maximum.

According to the experimental data presented in Figures B.4-1 and B.4-2, the variation of initial pressure from 1 to 5 bar does not affect the turbulent combustion rate. The turbulent combustion rates behave in a similar way in hydrogen-air, hydrogen-air-steam, and hydrogen-air-carbon dioxide mixtures.

B. 5 Flammability Limits of H_2-Air-CO_2 Mixtures

Practical considerations of safety require knowledge of the flammability limits for H_2-air-CO_2 mixtures. As mentioned earlier, there is a lack of data for mixtures of H_2-air-CO_2 at elevated pressures. Most of the experimental work reported in literature has been conducted at room temperature and at atmospheric pressure. In the case of elevated pressure-temperature conditions, experimental data exhibit a great deal of scatter for high inert component fractions.

Effect of pressure on the flammability limits of hydrogen-air-carbon dioxide mixtures is studied using the bomb method for the flammability determination. The maximum percentage of hydrogen at a given percentage of carbon dioxide in a hydrogen-air-carbon dioxide mixture, for which ignition by a sufficiently powerful source (about 1 to 2 J) did not cause a noticeable increase in pressure, was used as the practical definition of the limit. Such an approach has been used for hydrogen-oxygen-steam mixtures at various pressures.

Figure B.5-1 shows the experimental data measured in the spherical bomb of 4.2 L with central ignition at two initial pressures of 1 and 5 bar at 298 K . Ignition energy is equal to about 2 J. These data are presented on the domain (%CO_2) ÷ (% H_2) and are compared with the experimental data on the flammability limits by Coward and Jones [B.3] .Maximum pressures on combustion are shown in Tables B.5-1 and B.5-2.

It is apparent that the pressure rise from 1 bar to 5 bar diminishes the flammability of H_2-air-CO_2 mixtures in the vicinity of the quenching point. The lean branch of the flammability curve measured here coincides with the data obtained by Coward and Jones [B.3] . Measured limiting percentage of CO_2 is equal 57.6% by volume at atmospheric pressure and 51.2% at 5 bar.

B.6 Detonability of Hydrogen-containing Mixtures with CO_2, H_2O, and N_2 Additives

Detonation limits exist in tubes because of interaction between the flow in the reaction zone and tube walls. In a tube that is smaller in diameter than a certain limiting value (limiting tube diameter - D*) self-sustaining detonation becomes impossible. The computation of D* for detonation in hydrogen-contained air mixtures is described in Reference [B.4]. These results were compared with available data and experimental results in tubes of 24 mm and 41 mm inner diameter .The agreement between the calculated and the measured value of D* was good. Therefore, the same method and detailed kinetic scheme were used for limits of detonability in H_2-CO-air mixtures and multi-component H_2-CO-CO_2-H_2O-air systems relevant to accident scenario in a pressured-water reactor (PWR) .A distinguishing feature of the multi-component H_2–CO–CO_2–H_2O-air system is two different combustible gases, namely, H_2 and CO_2 in mixture. It is reasonable to display experimental and theoretical results for such a system with the help of a percent H_2 and a percent CO_2 diagram.

Shown in Figures B.6-1 (a) and (b) are examples of computation of detonability curves for H_2–air –CO_2 and H_2-air–H_2O mixtures in a tube of 41 mm diameter . A triangular domain is formed as a result of this computation . A inner part of this domain corresponds to detonable mixtures. The results of limiting concentration measurements at initial pressure p_0 = 1 bar and temperature T_0 = 298 K and 373 K for H_2-air–CO_2 mixture are plotted on the graph by open and solid squares .The increase of initial temperature tends to enlargement of the detonability area . The mitigation effect of steam is less than that of carbon dioxide. The influence of the tube's diameter on the detonability is conveniently illustrated in a diagram. Figure B.6-2 shows the limiting concentrations of H_2 and H_2O (the rest being air) for tubes of 10 mm, 41 mm and 300 mm inner diameter and at initial temperature 373 K. Kumar′s experimental data [B.5] plotted (as a dotted line) for the flammability limits of the same mixtures shown relevant downward flame propagation.

Shown in Tables B.6-1 to B.6-3 are the concentrations of hydrogen and additive (CO_2 or N_2) in characteristic points of detonability diagrams. The points *A* and *B* correspond to lean (lower) and rich (upper) limits for non-diluted mixtures. The point *C* corresponds the *nose * of the detonability domain. The narrowing of the region of detonability in the case of dilution with nitrogen is accounted for in Figure B.6-3 by an upper branch. A lower branch of detonability curve does not change at dilution with N_2 up to 50% N_2.

The flammability limits can coincide with the detonability limits predicted for mixtures with large amounts of hydrogen. This coincidence is likely if tube diameter is great. In narrow channels the detonability area is narrower than the flammability area.

Specific features of detonability of mixtures with two-component fuel were verified by use H_2+ Air + CO + CO_2 systems . Figure B.6-4 shows the detonability diagram for that case. Percentage of CO_2 diluent is used as a parameter and percentage of air is known from material balance. The detonability domain at given tube diameter has the form of a * peninsula * with size dependent on amount of diluent in the mixture . Experimental points [B.4, B.13] are plotted on the diagram for case of undiluted mixture (solid circles) and for the variant of dilution by 10% CO_2 (solid squares). Calculated and measured data at p_0 = 1 bar and T_0 = 298 K show a reasonable agreement .The additional combustible gas (carbon monoxide) decreases the limiting concentration of hydrogen in the mixture proportionally the carbon monoxide concentration. This proportionality exists at small additions of CO to hydrogen. An additional set of the experimental data about limiting conditions of detonation propagation in tubes of different size is presented in Tables B.6-4 to B.6-7.

B.7 Ignition Limits of H_2 + Air + CO_2 and H_2 + Air + H_2O Mixtures by a Hot Gas Jet

The ignition limits of hydrogen–air mixtures diluted with steam or carbon dioxide have been studied as a function of mixture composition [B.14]. Ignition was produced by a hot transient jet emerging from the downstream end of a shock tube and entering a combustion chamber. The spurted gas was heated by a reflected shock wave between 750 K and 2800 K. The ejection velocity was subsonic. With an initial jet at 2600 K, the ignition area of H_2-air-CO_2 mixtures was larger than that of the H_2-air-H_2O mixtures. The ignition area was located inside the flammability range of these systems for rich mixtures. On the contrary, ignition limits and flammability limits were almost similar for lean mixtures.

B.8 References

[B.1] Laminar and Turbulent Flame Propagation in H_2 + Air + Steam Mixtures at Accident Relevant Pressure @ Temperature Conditions, ICh Ph RAS at INR FZK Research Report, 1995.

[B.2] Laminar and Turbulent Flame Propagation in H_2 + Air + CO_2 Mixtures at Accident Relevant Pressure @ Temperature Conditions, IChPh RAS at INR FZK Research Report, 1996.

[B.3] Coward and Jones

[B.4] B. Lewis and G. Elbe, Combustion, Flames and Explosions in Gases, 3rd ed., Academic Press, 1987, 739 p.

[B.5] G.L .Agafonov, O.E. Popov, A.Yu. Kusharin and B.E. Gelfand, Detonability of H_2 / CO / CO_2 / AIR mixtures, Combustion Science and Technology, Vol 135, 85–96, 1998.

[B.6] R.K. Kumar, Flammability limits of $H_2 – O_2$ – Diluent Mixtures, Journal of Fire Sciences, Vol 3, 1985, 245-262.

[B.7] G. Ciccarelli , J.L. Boccio, T. Ginsburg , C. Finfrock, L. Gerlach, K. Sato and A.M. Kinoshita, High-Temperature Hydrogen + Air + Steam Detonation Experiments in the BNL Small-scale Development Apparatus, BNL-NUREG-52414, NUREG /CR-6213, 1994.

[B.8] G. Ciccarelli , T. Ginsberg , J.L. Boccio , C. Finfrock , L.Gerlach and H. Tagawa, Detonation Sell Size Measurements of High Temperature H_2 + Air + Steam Mixtures, BNL-NUREG-52482, NUREG/CR–6391, 1997.

[B.9] S.R . Tieszen , M.P. Sherman , W.D. Benedick and J.E. Shepherd, Detonation Sell Size Measurements in H_2 + Air + Steam Mixtures, Progress in Astronautics and Aeronautics, AIAA Inc., NY, Vol 106, 1986, 205.

[B.10] Evaluation of H_2-Contained Mixtures Detonability, Report of IchPh RAS at INR FZK, 1996.

[B .11] W. Jost and H.Gg .Wagner, Influence of Various Parameters on Initiation, Stability and Limits of Detonation, AFOSR-78-35871979; AFOSR-79-0117A , 1981; AFOSR-TR-69-09, 1969.

[B.12] S.R . Tieszen, P.S . Martin, W.B. Benedick and M. Berman, Detonability of H_2- Air –Diluent Mixtures, NUREG/CR-4905, SAND–85-1263, 1986.

[B. 13] D.W. Stamps, W.B. Benedick and S.R. Tieszen, Hydrogen-Air–Diluent Detonation Study for Nuclear Reactor Safety Analyses, NUREG/CR-5525 SAND–89-2398, 1991.

[B.14] Detonability of Hydrogen-Containing Mixtures Under Conditions Relevant to PWR Accident Scenarios, ICh Ph RAS at INR FZK Research Report,1994.

[B.15] N. Djebaili, R Lisbet, C. Paillard and G. Dupre, Comparison Between Ignition of H_2–Air– O_2 and H_2–Air-H_2O Mixtures by a Hot Gas Jet, Shock waves @ Marseille, 2 , Proc. 19th ISSW (ed. R.Brun and L. Dumitrescu),1995, 149-154.

Table B.2-1 Laminar burning velocities in lean H_2-air-CO_2 mixtures

f	**%H_2**	**%CO_2**	**S_u (cm / s)**		
			1 bar	**3 bar**	**5 bar**
0.21	8	-	3.3		
0.21	7.6	5.0	2.1		
0.21	7.2	10	2.0		
0.26	10	-	20.2		
0.26	9.5	5	9.9		
0.26	9.0	10	6.5		
0.26	8.2	17.8	4.3	4.1	3.5
0.39	14	-	54		
0.39	12.6	10	30		
0.39	11.2	20	15		
0.39	9.8	29.7	3.3	3.7	3.4
0.59	17	15	69		

Table B.3.2–1 Pressure exponents for lean H_2-Air-CO_2 mixtures

Pressure range, bar	**f = 0.39; 10% CO_2**		**f = 0.39; 20% CO_2**		**f = 0.26; 5% CO_2**	
	298 K	**393 K**	**298 K**	**393 K**	**298 K**	**393 K**
1 - 3	-0.32	-0.30	-0.46	-0.42	-0.46	-0.44
3 - 5	-0.43	-0.43	-0.72	-0.59	-1.1	-0.59

Table B. 3.3-1 Temperature exponents for lean H_2-air-CO_2 mixtures

Temperature range, K	**f = 0.39; 10% CO_2**			**f = 0.39; 20% CO_2**			**f = 0.26; 5% CO_2**		
	1 bar	3 bar	5 bar	1 bar	3 bar	5 bar	1 bar	3 bar	5 bar
298 - 473	2.8	2.9	2.9	3.1	3.1	3.2	3.6	3.6	4.1

Table B.5-1 Relative pressure rise in H_2-air-CO_2 mixtures at T_o = 298 K and P_o = 1 bar

H_2 , %	5.0	5.3	6.0	6.55	7.2	8.0	8.9	10.9	15.0
CO_2 , %	33.2	50.0	53.4	55.2	56.4	57.6	57.6	55.6	52.0
$(P_e / P_o)_{exp}$	1.04	1.04	1.02	1.02	1.02	1.03	1.03	1.07	1.07

Table B.5–2 Relative pressure rise in H_2-air-CO_2 mixtures at T_o = 298 K and P_o = 5 bar

H_2 , %	5.45	6.55	8.0	8.95	15.0
CO_2 , %	46.4	50.4	51.2	50.4	44.8
$(P_e / P_o)_{exp}$	1.01	1.02	1.01	1.10	1.71

Table B.6-1 Percentage of H_2 and $C0_2$ (or N_2) in the characteristic points of the detonability diagrams in hydrogen-air-diluent mixtures at 298 K

Initial pressure, bar	**A, %H_2**	**B, %H_2**	**C, CO_2**	**C, %N_2**
Tube diameter d = 2 cm				
1	18.0	57.8	113	35.0
3	18.8	60.0	13.3	35.0
5	18.2	61.6	15.2	36.9
Tube diameter d = 100 cm				
1	12.7	73.8	29.2	56.9
3	12.0	75.7	32.7	57.7
5	11.7	76.7	34.4	60.2

Table B.6-2 Percentage of H_2 and $C0_2$ (or N_2) in the characteristic points of the detonability diagrams in hydrogen-air-diluent mixtures at 400 K

Initial pressure, bar	A, %H_2	B, %H_2	C, CO_2	C, %N_2
Tube diameter d = 2 cm				
1	14.3	64.4	160	46.3
3	16.1	65.7	173	44 1
5	16.0	67.1	19.2	44.8
Tube diameter d = 100 cm				
1	10.4	78.8	347	65.0
3	10.2	80.5	38.3	65.6
5	9.8	81.5	40.1	66.8

Table B.6-3 Percentage of H_2 and C0$_2$ (or N_2) in the characteristic points of the detonability diagrams in hydrogen-air-diluent mixtures at 500 K

Initial pressure, bar	A, %H_2	B, %H_2	C, CO_2	C, %N_2
Tube diameter d = 2 cm				
1	10.9	70.0	21.7	56.2
3	13.1	71.5	22.1	567
5	13.6	72.5	23.8	53.6
Tube diameter d = 100 cm				
1	7.9	837	41 3	73 4
3	7.9	84.6	45.0	72.3
5	7.8	85.5	46.8	73.2

Table B.6-4 Near-detonability limit mixtures in tube Æ 100 mm [B.6]

Test[1]	% H_2	% H_2O	T [K]	Regime
312	30.27	24.77	500	DH
223	30.01	30.01	500	SH
314	29.92	19.96	300	DH
316	29.92	24.95	300	SH
148	16	-	300	DH
255	15	-	300	SH
284	12.04	-	500	DH
288	11.58	-	500	DH
348	9	-	650	DH
375	9	-	650	SH

DH – double-head detonation, **SH** – single-head detonation

Table B.6-5 Near-detonability limit mixtures in tube Æ 273 mm [B.7]

Test [1]	% H_2	% H_2O	T [K]	Regime
308	29.37	50	650	SH
310	17.26	30	650	DH
385	18.21	20	400	SH
389	9.86	15	650	SH
327	7.02	-	650	DH
317	7.39	-	650	SH
302	6.24	-	650	SH
110	9.9	-	500	DH
25	14.31	-	300	DH
232	13.83	-	300	DH
233	13.48	-	300	DH

DH – double-head detonation , **SH** – single-head detonation

Table B.6-6 LDL and RDL in H_2 + air mixtures

D	LDL	RDL	Ref.	Lab.
mm	% H_2	% H_2	-	-
100	15	-	[B.6]	BNL
273	13.5	-	[B.7]	BNL
430	13.5	70	[B.8]	SNL
300	13.5	70	[B.8]	Mc Gill
41	19	-	[B.9]	IchPh @ FZK
26	15	61	[B.0]	GU

Table B.6-7 LDL and RDL in SNL tests [B.6, B.7]

D	T	LDL	RDL	Ref.
Mm	[K]	% H_2	% H_2	-
430	293	13.5	70	[B.8, B.11]
430	373	13	-	[B.8, B.11]
430	293	11.6	74.9	[B.12]
430	373	9.4	76.9	[B.12]

LDL- lean detonability limit, **RDL** – rich detonability limit

BNL – Brookhaven National Laboratory (USA), **SNL** – Sandia National Laboratory (USA), **McGill** – McGill University (Canada) , **I ChPCh** – Institute of Chemical Physics RAS (Russian Federation) , **GU** – Göttingen university (Germany), **FZK** – Research Center Karlsruhe (Germany)

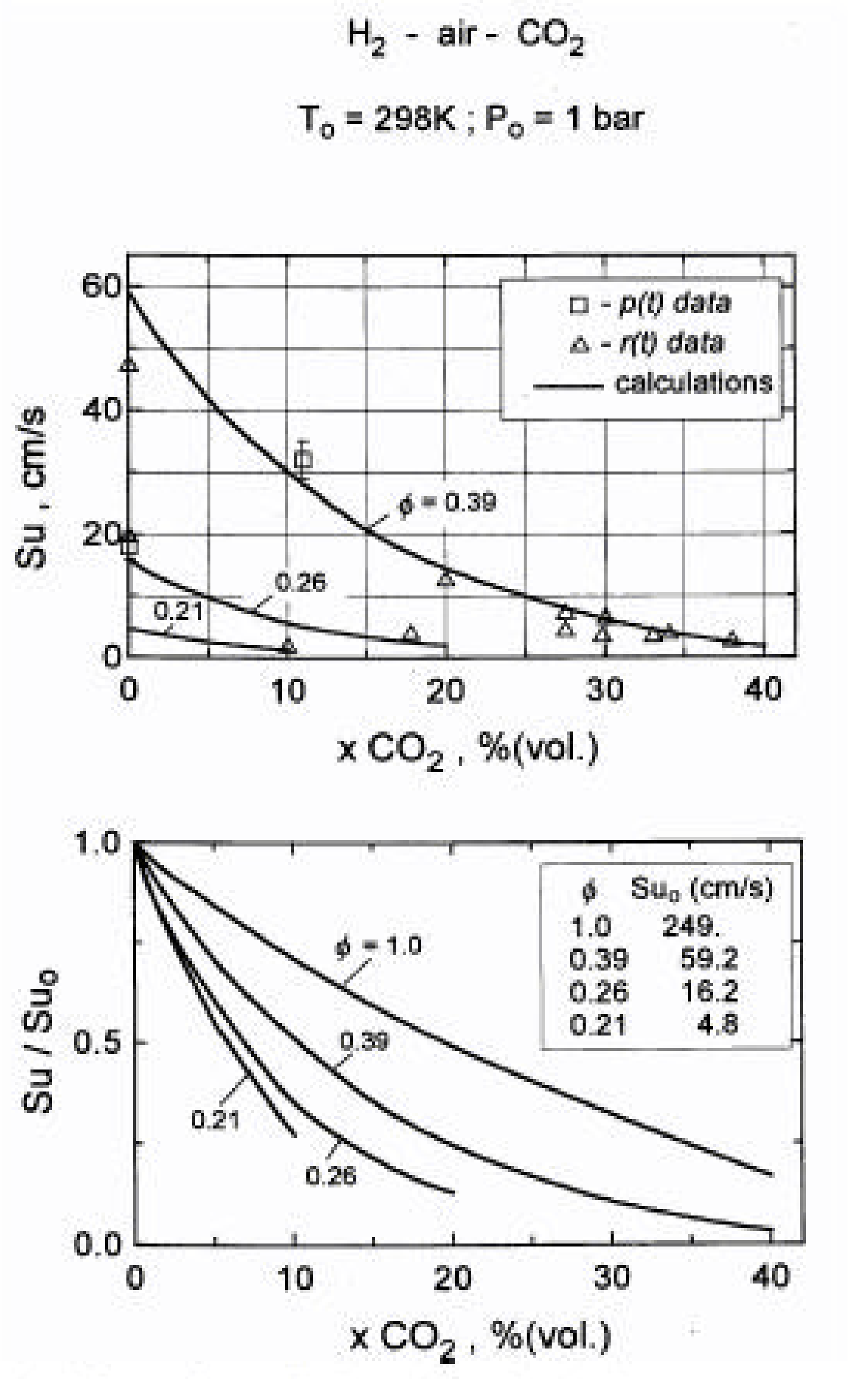

Figure A.2.1. The influence of CO_2 – dilution on the burning velocity

Figure B.3.1-1 The influence of CO_2 dilution on the burning velocity

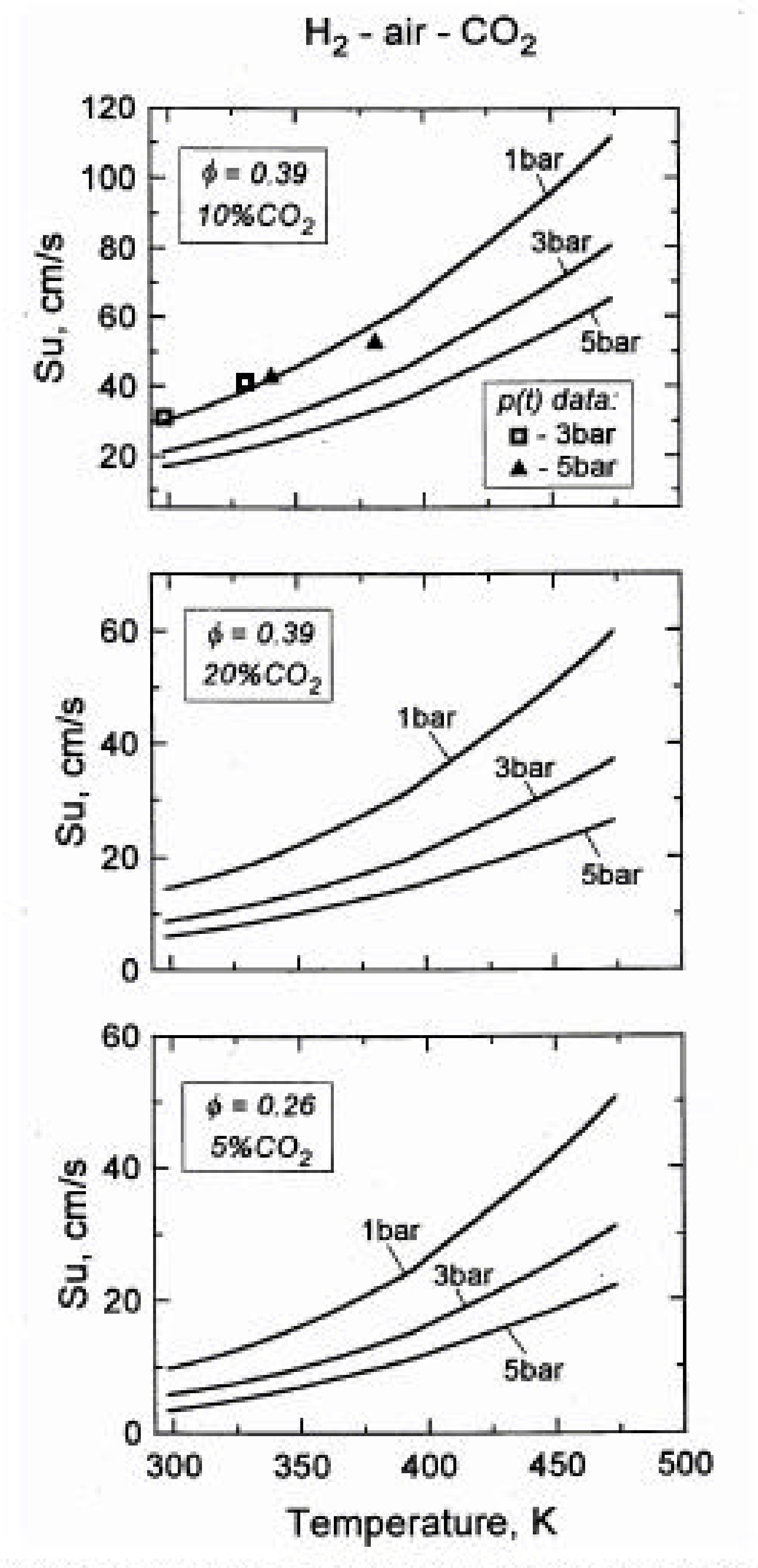

Figure A.2.3. The influence of temperature on the burning velocities in the H_2-air-CO_2 mixtures.

Figu
mixt

Figure B.3.3-1 The influence of temperature on the burning velocities in the H_2-air-CO_2 mixtures

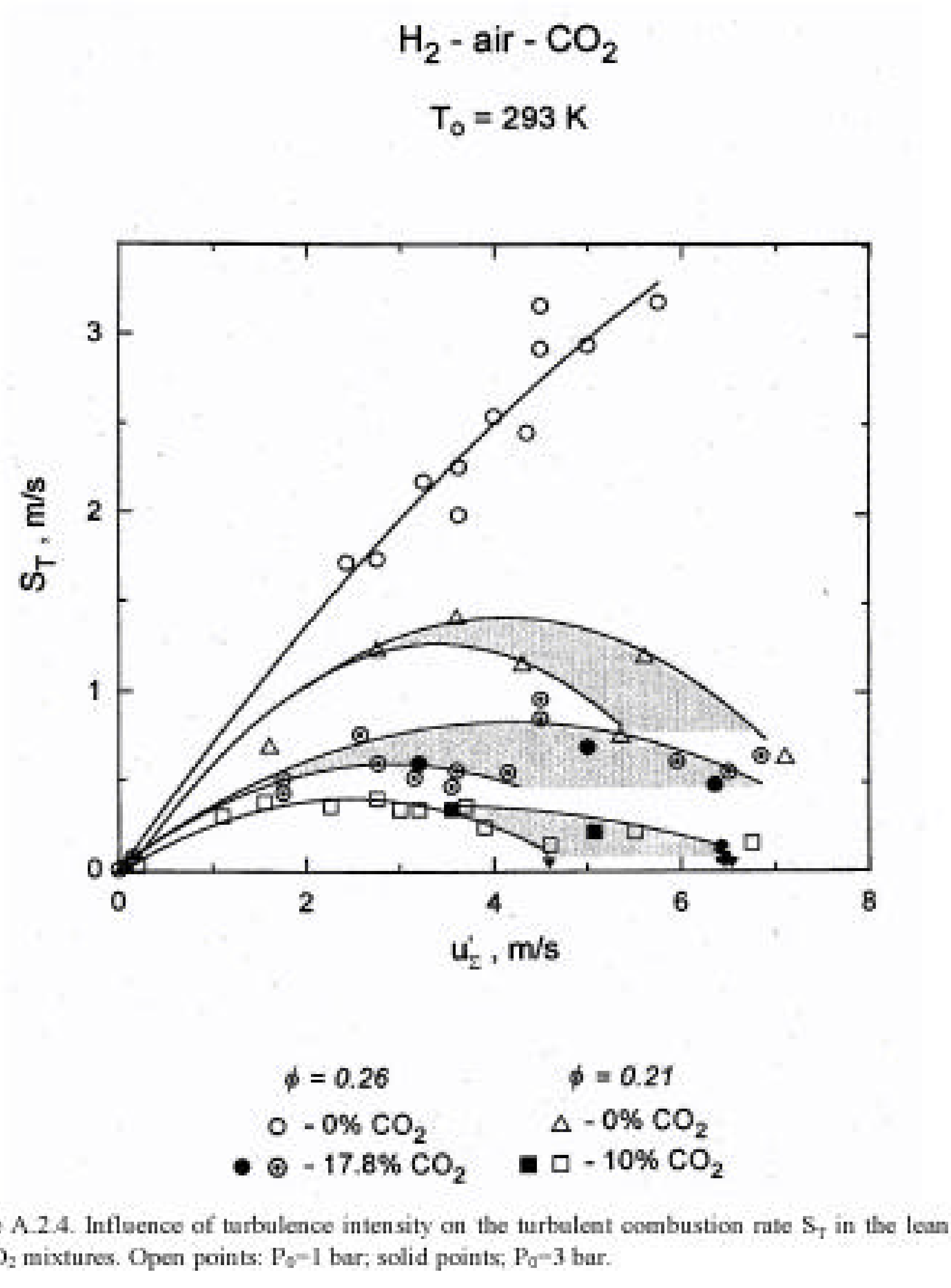

Figure A.2.4. Influence of turbulence intensity on the turbulent combustion rate S_T in the lean H_2-air-CO_2 mixtures. Open points: P_0=1 bar; solid points; P_0=3 bar.

Figure B.4-2 Influence of turbulence intensity of the turbulent combustion rate S_T in the lean H_2-air-CO_2 mixtures. Open points: P_0 = 1 bar; solid points; P_0 = 3 bar.

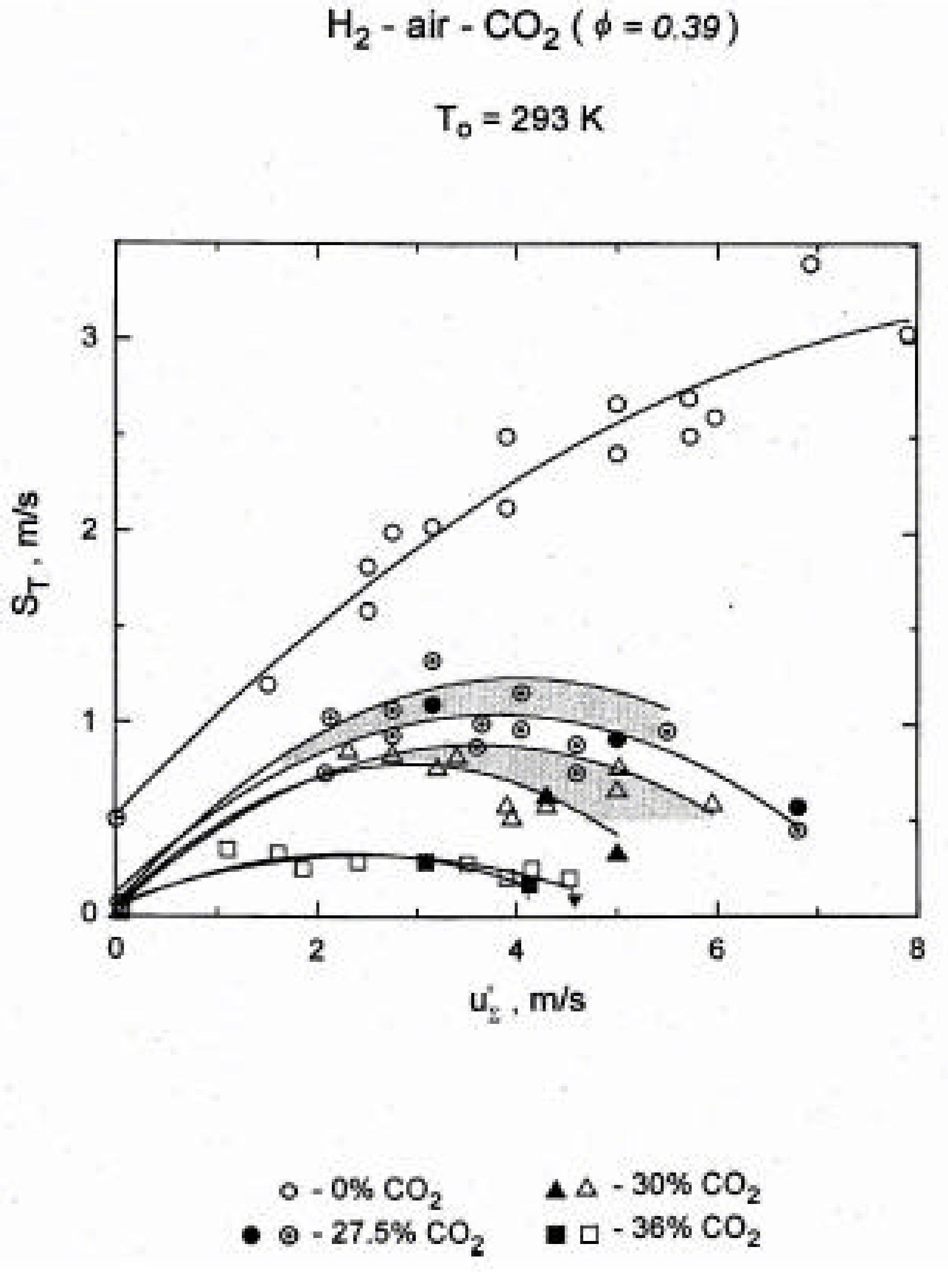

Figure A.2.5. Influence of turbulence intensity on the turbulent combustion rate S_T in the lean H_2-air-CO_2 mixtures. Open points: P_0=1 bar; solid points; P_0=5 bar.

Figure B.4-1 Influence of turbulence intensity on the turbulent combustion rate S_T in the lean H_2-air-CO mixtures. Open points: P_0 = 1 bar; solid points: P_0 = 5 bar.

Figure B.5-1 The influence of initial pressure on the flammability limits in H_2-air-CO_2 mixtures

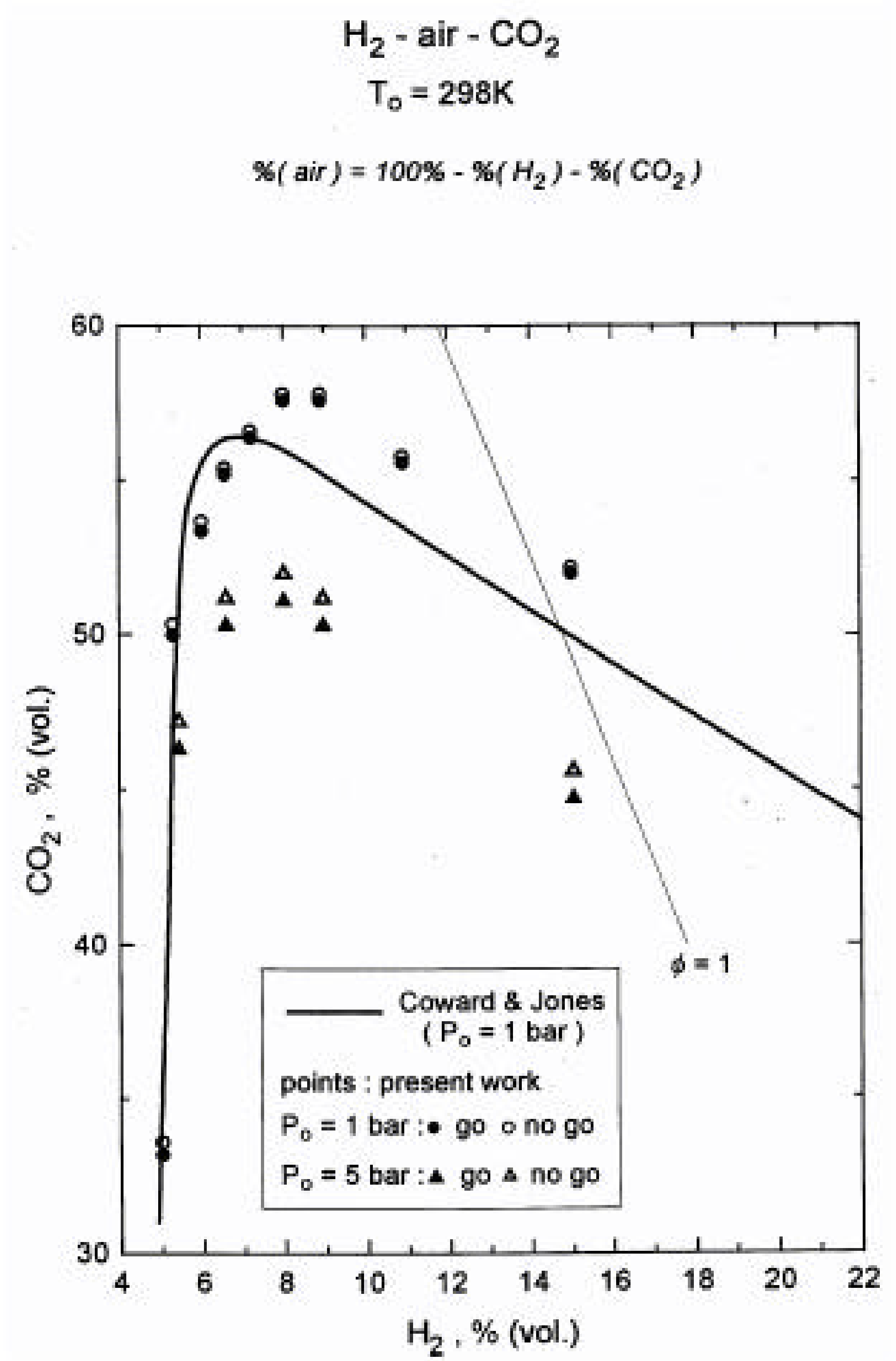

Figure A.2.6. The influence of initial pressure on the flammability limits in H_2-air-CO_2 mixtures.

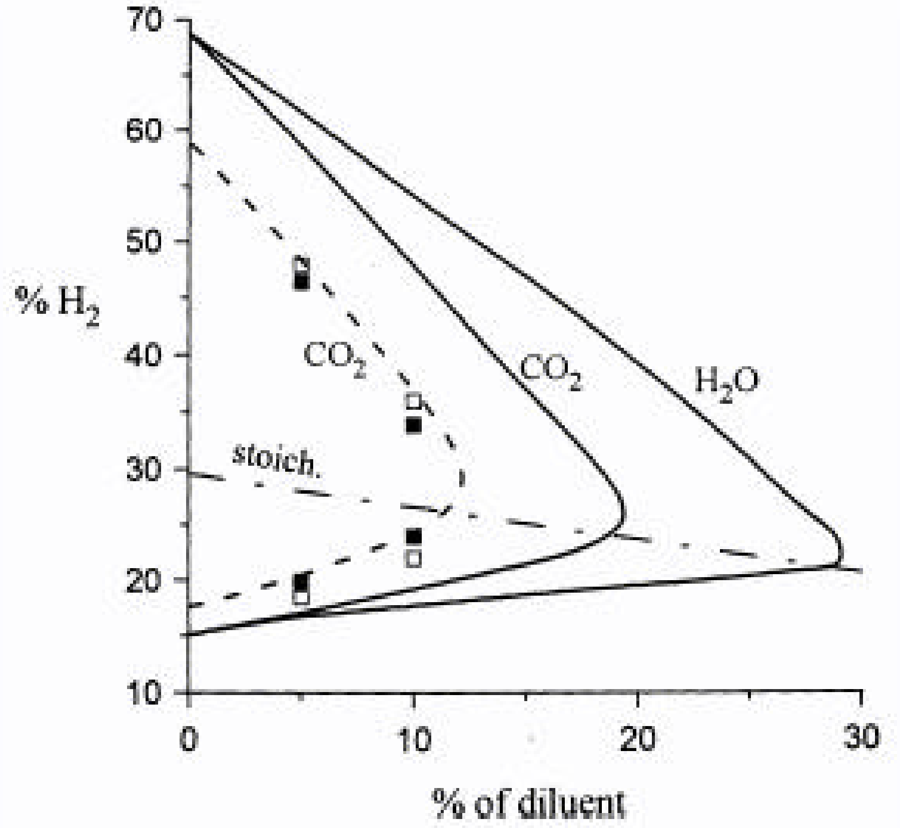

Figure A.2.7(a). Detonability diagram for H_2 + Air +CO_2 and H_2 + Air + H_2O mixtures at fixed tube diameter 41 mm.

Solid lines:T_0=373K; ρ_{air}=41.6mole/m^3.

Broken lines : T_0 = 298 K , P_0 = 1 bar.

Points: ■ - go , □- no go.

Figure B.6-1a Detonability diagram for H_2 + air + CO_2 and H_2 + air + H_2O mixtures at fixed tube diameter 41 mm

Solid lines: T_0 = 373 K; r_{air} = 41.6 mole/m^3.

Broken lines: T_0 = 298 K; P_0 =1 bar.

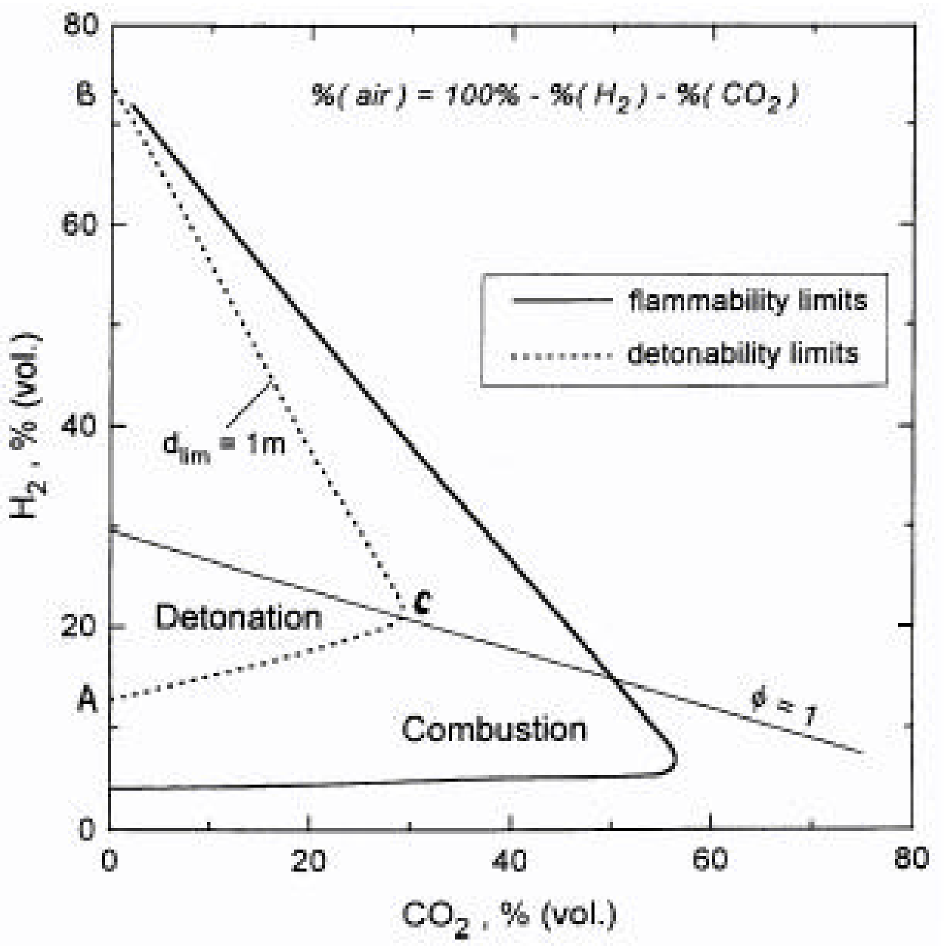

Figure A.2.7(b). Effect of CO_2 on suppression of detonation and deflagration in H_2 + Air mixtures.

Figure B.6-1b Effect of CO_2 on suppression of detonation and deflagration in H_2 + air mixtures

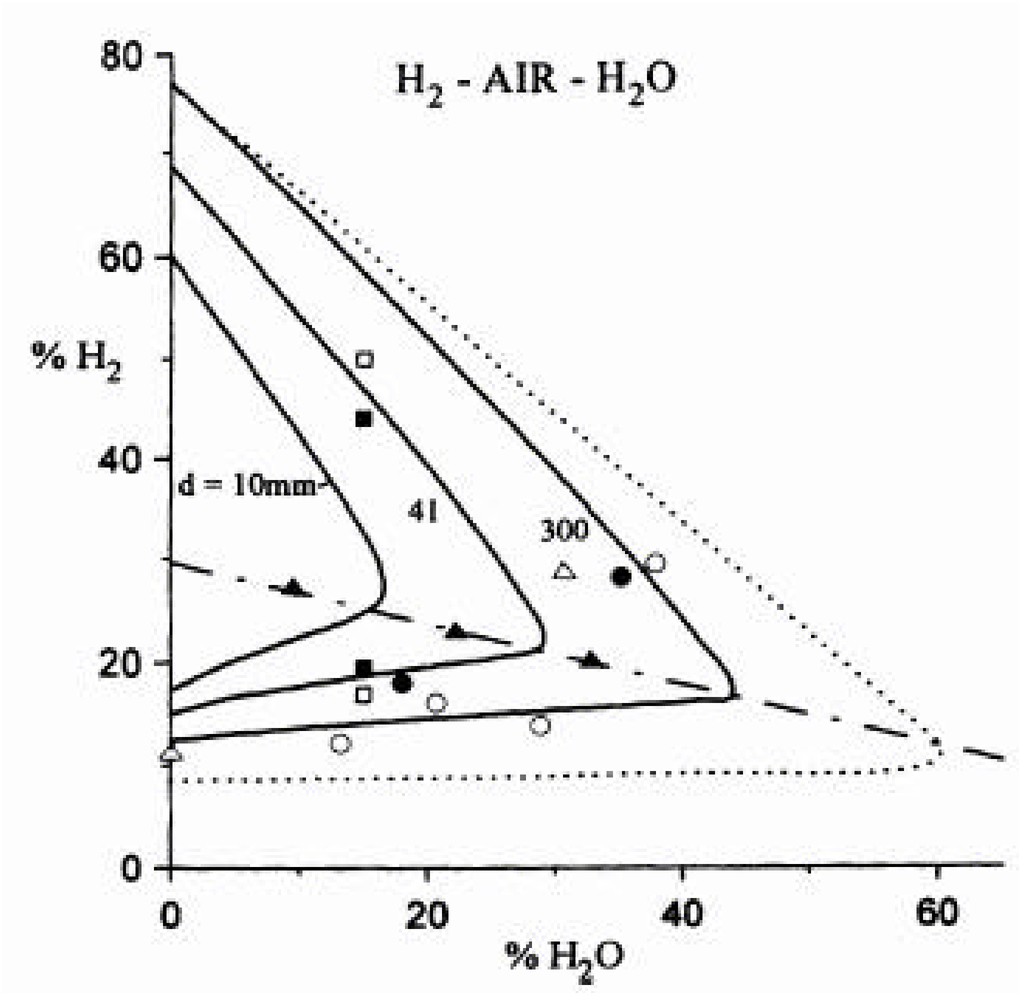

Figure A.2.8. Detonability diagram (solid lines) for H_2 + Air + H_2O mixtures. Calculations for different tube diameters: $T_0 = 373$ K : $\rho_{air} = 41.6$ mole/m^3 .

Points : measurements for d = 41 mm ; ■ - go , □ - no go.

Dotted line : experimental data for downward flame propagation limits at sub-atmospheric pressure $P_0 = (0.2 \div 0.5)$ bar.

NUREX - 6213 (d=100 mm) ▲ - go △ - no go

NUREG - 6391 (d=270 mm) ● - go ○ - no go

Figure B.6-2 Detonability diagram (solid lines) for H_2 + air + H_2O mixtures. Calculations for different tube diameters: T_0 = 373 K; r_{air} = 41.6 mole/m^3.
Points: measurements for d = 41 mm;
Dotted line: experimental data for downward flame propogation limits at sub-atmospheric pressure P_0 = (0.2 ¸ 0.5) bar.
NUREX = 6213 (d = 100 mm)
NUREG = 6391 (d = 270 mm)

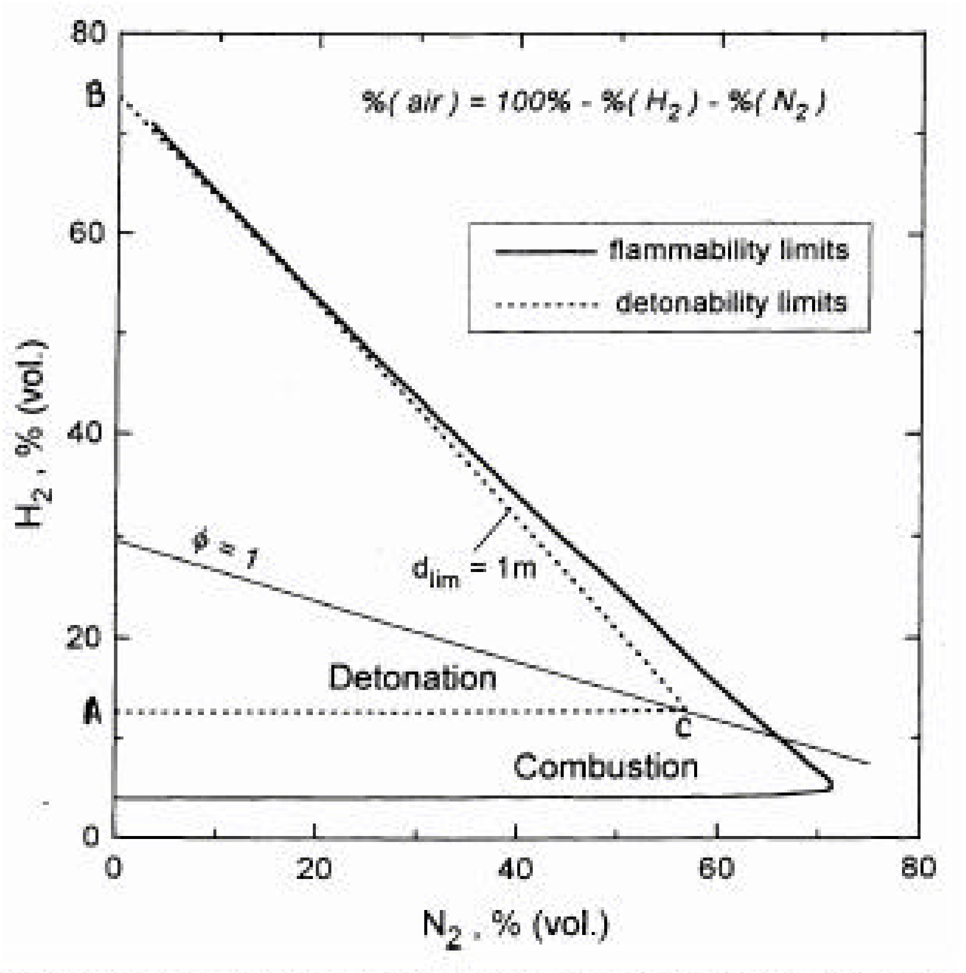

Figure A.2.9. Effect of N_2 on suppression of detonation and deflagration in H_2 + Air mixtures.

Figure B.6-3 Effect of N_2 on suppression of detonation and deflagration in H_2 + air mixtures

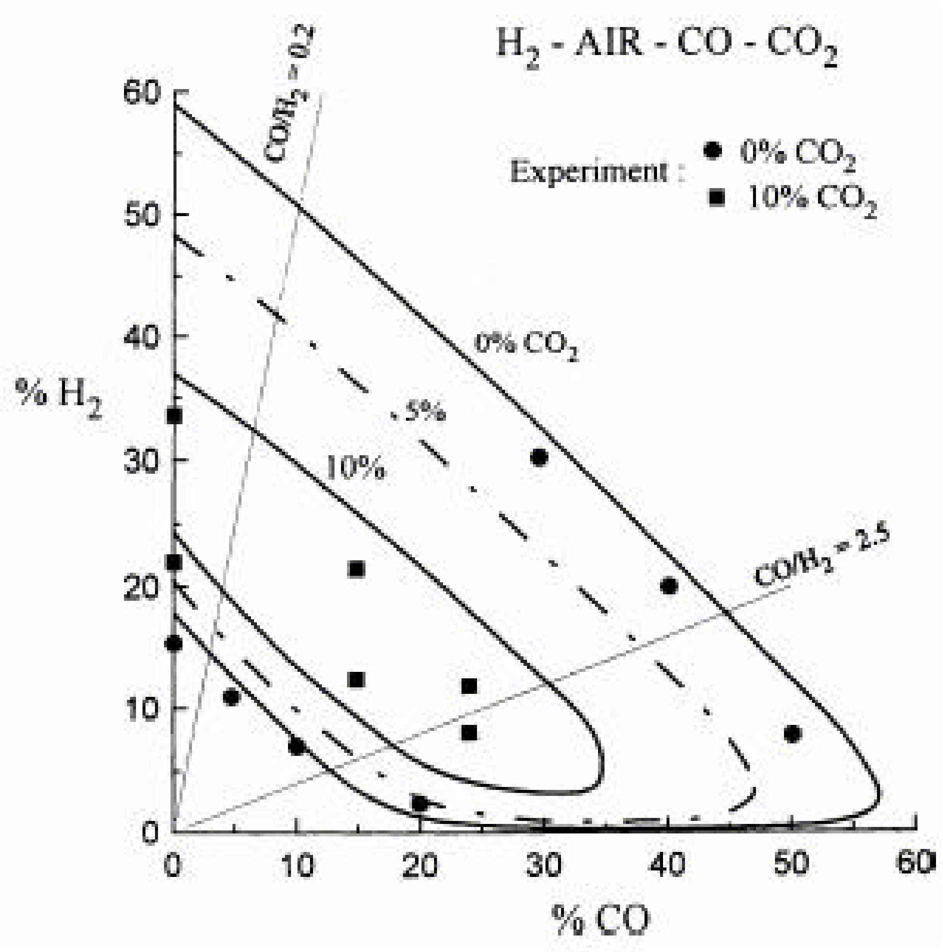

Figure A.2.10. Detonability diagram for H_2 + Air + CO + CO_2 mixtures with two-component fuel at fixed tube diameter 41 mm. Comparison of calculated and measured data at T_0 = 298 K, P_0 = 1 bar .

Figure B.6-4 Detonability diagram for H_2 + air + CO + CO_2 mixtures with two-component fuel at fixed tube diameter 41 mm. Comparison of calculated and measured data at T_0 = 298 K, P_0 = 1 bar.